Wind Engineering Joint Usage/Research Center
FY2021 Research Result Report

Research Field: Wind Hazard Mitigation
Research Year: FY2021
Research Number: 21213001
Research Theme: Wind pressure distribution on multi-slope and multi-level roofs of low-rise light-weight steel residential buildings

Representative Researcher: Y. Q. Li

Budget [FY2021]: 350000Yen

1. Research Aim

Up to now, low-rise light-weight steel residential buildings with cold-formed thin-walled steel sections are widely used in the world, as well as in China, due to its excellent suitability to industrialized construction [1, 2]. Usually, the architecture shape of the roofs is much more flexible, for example, with multi-slopes and multi-levels (Fig.1.1). Normally in wind-resistant design, for the roofs with single slope, double slopes, even four slopes, the wind pressure coefficients distribution on the roofs can be referred from the corresponding load codes [3-7]. For other roofs with multi-slopes, and even multi-levels, there is no enough and reliable information of wind pressure coefficients distribution for wind-resistant design in practice. However, wind-resistant design is critical to the economy of the roofs for such kind of low-rise light-weight steel residential buildings. Therefore, investigation on wind pressure coefficients distribution of typical multi-slope and multi-level roofs is one of the key issues and a challenge for wind-resistant design of low-rise light-weight steel residential buildings.

Fig. 1.1 Low-rise residential buildings with multi-slope and multi-level roofs

The research aim of this project is to investigate effect of multi-slope and multi-level shape on wind pressure distribution on typical roofs of low-rise light-weight steel residential buildings.

2. Research Method

Wind tunnel tests and CFD simulation would be used in the study, including: 1) CFD simulation on wind pressure coefficients distribution of typical multi-slope and multi-level roofs will be carried out to understand the “important” difference for the “special” slopes of the roofs, so that the design of BLWT

models can be instructed for further investigation; 2) Wind tunnel tests on typical rigid models of low-rise residential buildings with typical multi-slope and multi-level roofs in BLWT of TPU with a basic model considering the important no dimensional parameters; 3) Analysis and suggestion of wind pressure coefficients distribution of low-rise residential buildings with typical multi-slope and multi-level roofs.

However, due to the continuous epidemic situation of COVID-19 in both China and Japan, international travelling is impossible, and the planned BLWT tests had to be cancelled, and only CFD simulation was conducted finally, and the main investigation includes: (1) selecting the internationally recognized Silsoe Cube standard test model as a reference, conducting CFD simulations, comparing the CFD simulation results with existing test data, and verifying the accuracy and validity of the CFD simulation; (2) designing the shape parameters of building models with multi-slope and multi-level roof, determining the considering variables, the size of numerical calculation field and various parameters in CFD simulation; (3) using the method of CFD simulation to calculate the wind pressure distribution of each group of models with different shape parameters, and analyze the influence of different shape parameters on the wind pressure distribution of roofs of different parts.

3. Research Result

3.1 Calibration CFD simulation by Silsoe standard model

Before the formal numerical simulation for the multi-slope and multi-level roof models, the Silsoe cube model [8, 9] was selected to verify the accuracy and effectiveness of the numerical simulation.

The length of the cube, L, the width, B, and the height, H, are 6m. The sizes of calculation field are set as 25L long, 10B wide and 10H high, i.e., 150m (length) × 60m (width) × 60m (height). With the calculation field sizes, the actual blocking rate is 1%, which meets the requirement that the blocking rate should less than 3%.

Structured grid system is used for mesh generation of the computational field, and the mesh is refined on the surface of the model, so as to better capture the details of air flow near the model and on the surface. The result of mesh generation is shown in Fig. 3.1.

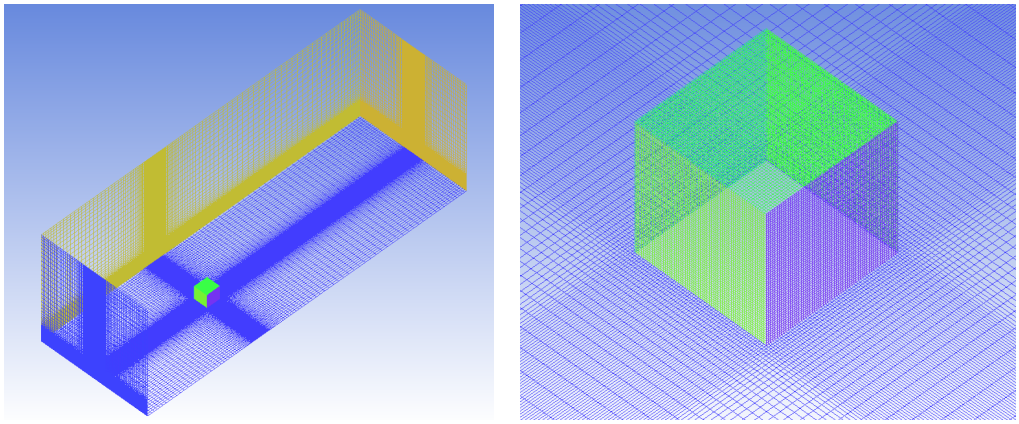

(a) Global (b) Local

Fig. 3.1 Structured grid for the Silsoe model

The inlet of the numerical simulation calculation field adopts the velocity inlet boundary condition, and the wind speed and the turbulence intensity profiles at the inlet are fitted and imported by User Defined Functions (UDF). The outlet adopts the outflow boundary conditions, both sides and top surfaces adopt the symmetry boundary conditions, and the ground and model surfaces adopt the rigid non-slip wall to simulate the ground and the model in the open area under the actual wind field environment.

3.1.1 Velocity and turbulence intensity profile

According to the existing field measured wind speed data, the logarithmic rate formula is used to fit the velocity profile:

$$\overline{U}(z)=\frac{u_*}{K}\ln(\frac{z}{z_0}) \tag{1}$$

where, u_*, K, and z_0 are the friction velocity, the Karman constant, and the roughness length, respectively.

According to the turbulence intensity formula under terrain category II in AIJ2015[6], the fitting turbulence intensity formula is selected as follows:

$$I(z)=\begin{cases}0.1\left(\dfrac{z}{z_G}\right)^{-\alpha-0.05} & z_b<z\le z_G\\ 0.1\left(\dfrac{z_b}{z_G}\right)^{-\alpha-0.05} & z\le z_b\end{cases} \tag{2}$$

where, α, z_b, and z_G are the ground roughness exponent, the interfacial layer height, and the gradient wind height under terrain category II.

The comparison among fitting velocity profile and turbulence intensity profile with wind tunnel test and field measurement results are shown in Figure 3.2:

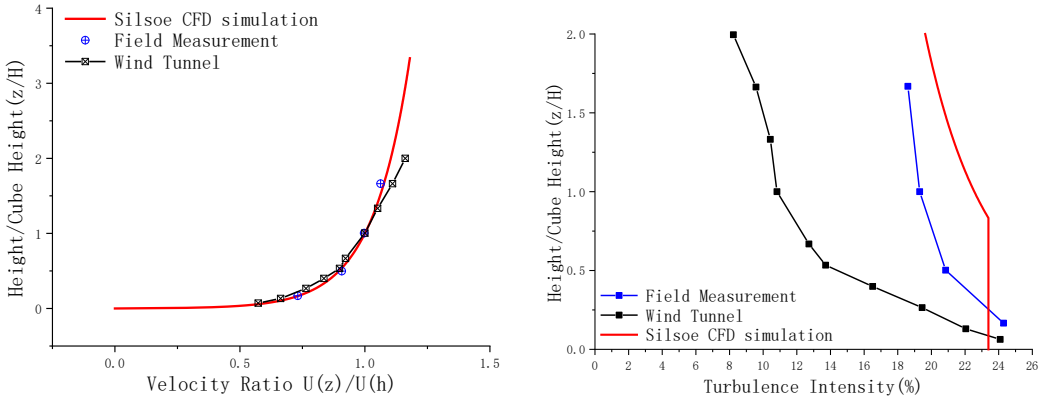

(a) Velocity (b) Turbulence intensity

Fig. 3.2 Comparison of fitting wind speed profile and turbulence intensity profile

3.1.2 Comparison of different turbulence models

In the CFD simulation, the reasonable selection of turbulence model is obviously important. In this project, different models, including the Standard k-ε, the RNG k-ε, the Realizable k-ε, the SST k-ω and the Reynolds Stress Model (RSM), are considered for the CFD simulation model of Silsoe Cube with the

same boundary conditions. The mean wind pressure coefficient is selected to judge the CFD simulation accuracy of different turbulence models. By comparing the mean wind pressure coefficient calculated by different turbulence models at a typical position with the field measurement results and wind tunnel test results, the influence of different turbulence models on the calculation results is summarized, and the turbulence model which is mostly in agreement with the actual situation is selected for the following simulation.

The formula of mean wind pressure coefficient is defined as follows：

$$C_p^i = \frac{2(p_i - p_0)}{\rho u_0^2}$$

where, C_p^i, p_i, p_0, ρ, and u_0 are the mean wind pressure coefficient at point *i*, the pressure at point *i*, the density of air, and the mean wind velocity at the reference point, respectively.

The comparison of wind pressure coefficients around the vertical central axis and the horizontal section at 3m high using different turbulence models with wind direction 90° are shown in Fig. 3.3.

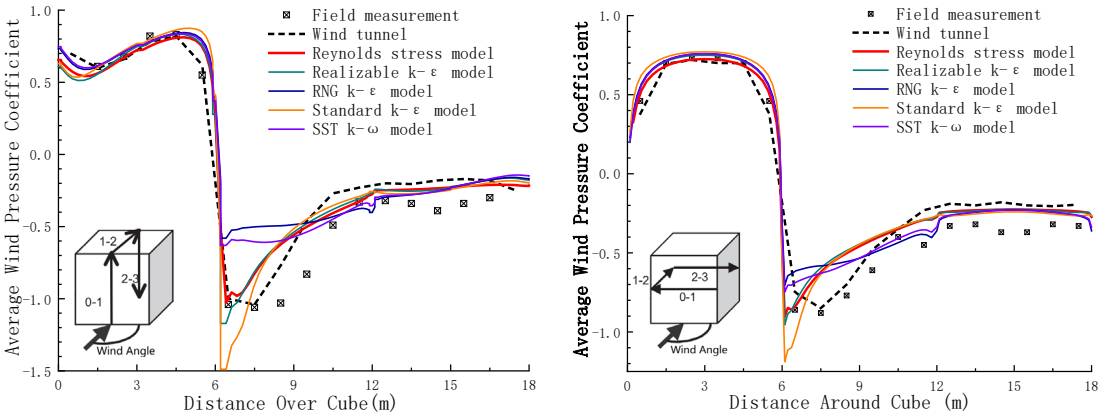

(a) Around the vertical central axis (b) Around the horizontal section at 3m high

Fig. 3.3 Comparison of wind pressure coefficients using different turbulence models

According to above comparison in Fig. 3.3, it can be found that, generally the calculation results using the Reynolds stress model and the realizable k-ε model are mostly close to those of wind tunnel test and field measurement, even there is only a little difference in the windward corner.

On the windward side of the model, the calculated results of each turbulence model are highly consistent with the wind tunnel test and field measurement results. The mean wind pressure coefficient calculated by the standard k-ε model is relatively high, but the simulation results of each turbulence model are generally satisfactory. At the top of the model, because of the strong separation and reattachment of airflow at the eaves of the roof, the airflow pattern is complex, so it is difficult to simulate it, and the accuracy or suitability of turbulence models is required, so the simulation results of each turbulence model are quite different from each other. Among all the turbulence models, the calculation error of standard k-ε model is particularly larger, and the absolute negative pressure appears at the windward angle, while the RNG k-ε model and SST k-ω model underestimate the negative pressure. Although Reynolds stress model can

simulate the wind pressure coefficient at the windward angle very well, it also has low negative pressure near the leeward angle. Generally speaking, Reynolds stress model has the best simulation result at the top of the model. On the leeward side, since the wind speed is low, the flow is not intense, and the calculation results of different turbulence models have little difference, which is in good agreement with the results of wind tunnel test and field measurement.

To sum up, because the simulation results of Reynolds stress model are much close to those of wind tunnel test and field measurement, it will be used for CFD simulation in this study.

3.2 Parameter settings in CFD simulation

3.2.1 Model parameter for typical building models with multi-slope and multi-level roofs

Many aspects are considered for typical low-rise residential building models with multi-slope and multi-level roofs in the study, including typicality to prototype buildings in geometry and main problems for wind load, flexibility and convenience for model fabrication for further wind tunnel test investigation with different cases, and convenience for CFD calculation. Finally, a module-based model is chosen as shown in Fig. 3.4, including a cuboid of 3m×3m×6m cuboid and an isosceles triangular prism with base-side of 6m, and the base edge of the triangular prism, i.e., three kinds of roof slope, 15°, 30° and 45°, is considered.

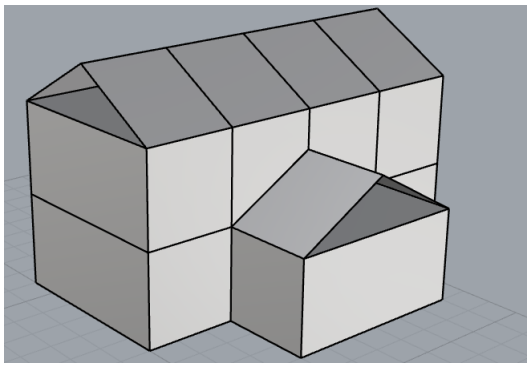

Fig. 3.4 Module-based models of typical buildings

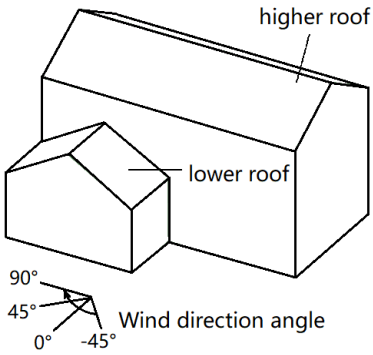

Fig. 3.5 Definition of wind angle

In order to study the similarities and differences of wind load distribution of multi-slope and multi-level roofs under different wind directions, CFD simulation is carried out for the wind direction of 0° , 45° , -45° and 90°, respectively. For the models with the low-rise buildings centrally arranged, only 45°is considered for comparison. The definition of wind direction is shown in Fig. 3.5.

Among different wind directions, the distribution of wind pressure coefficient on one-slope or double-slope roofs under 90° wind direction has recommended values in the codes related to wind load, such as *the design load code for building structures*, China[3]. The purpose of simulation under this condition is to verify whether there will be different, even unfavorable effect on both higher and lower roof surfaces under 90° wind direction. It should be noted that, the wind direction of 135° to -45° is not considered in the study since the wind pressure distribution on the windward side of the higher roof surface is similar to that of the simple double-slope roof, and the wind pressure coefficient on the lower roof surface, as on the leeward side, is relatively low usually.

The total models' information is listed in Table 3.1.

Tab. 3.1 Information of building models with multi-slope and multi-level roofs

No.	Model numbering	Arrangement of lower roof	Height of eaves	Length of lower roof	Roof slope	Wind direction
1-4	2FP1	Offset	6m	3m	30°	0°,45°,-45°,90°
5-7	2FZ1	Centered	6m	3m	30°	0°,45°,90°
8-11	2FP2	Offset	6m	6m	30°	0°,45°,-45°,90°
12-14	2FZ2	Centered	6m	6m	30°	0°,45°,90°
15-18	3FP1	Offset	9m	3m	30°	0°,45°,-45°,90°
19-21	3FZ1	Centered	9m	3m	30°	0°,45°,90°
22-25	3FP2	Offset	9m	6m	30°	0°,45°,-45°,90°
26-28	3FZ2	Centered	9m	6m	30°	0°,45°,90°
29-32	3FP1R15	Offset	9m	3m	15°	0°,45°,-45°,90°
33-35	3FZ1R15	Centered	9m	3m	15°	0°,45°,90°
36-39	3FP1R45	Offset	9m	3m	45°	0°,45°,-45°,90°
40-42	3FZ1R45	Centered	9m	3m	45°	0°,45°,90°

In Tab. 3.1 , 2F/3F means that the floor number of building part with higher roof is 2/3, i.e., one or two module in height , P1/P2 represents that the layout form of building part with lower roof -rise is offset and the length is 3/6 meters, i.e., one or two module size in length; Z1/Z2 means that the layout form of lower building part is centered and the length is 3/6 meters, i.e., one or two module size in length; R15/R30/R45 represents the roof slope is 15°, 30°and 45°, respectively. The total models used are shown in Fig. 3.6.

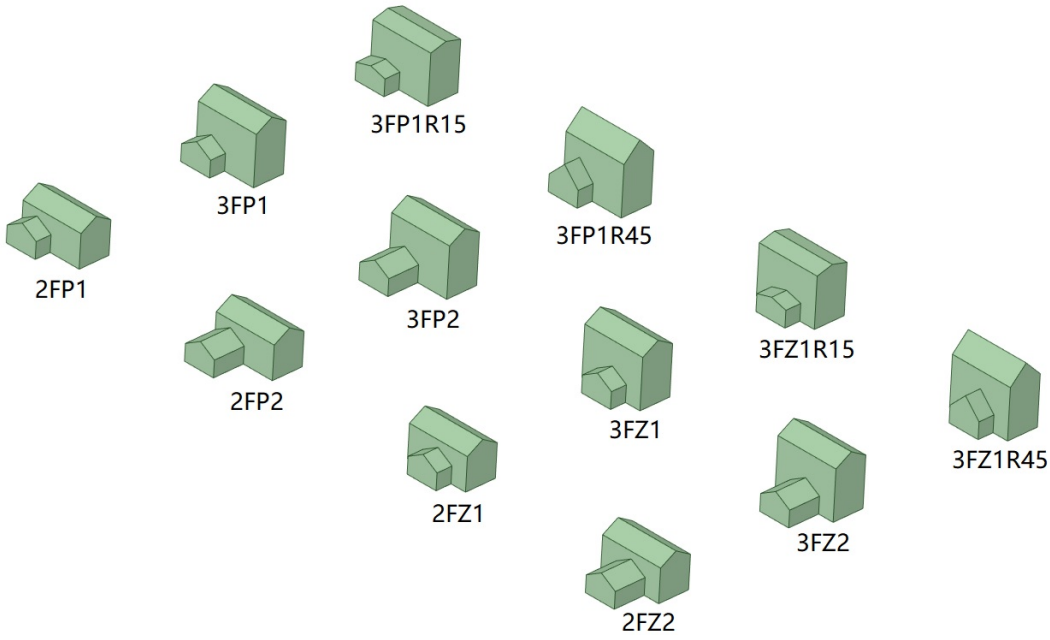

Fig. 3.6 Models with different parameters used in the study

3.2.2 Computing field and mesh generation

The maximum length, *L*, width, *B*, and height, *H*, of each model are 12m. Considering the blocking rate and calculation efficiency, the sizes of calculation field are set as 20*L* long, 8.33*B* wide and 5*H* high, i.e., *L*×*B*×*H*= 240m× 100m × 60m. Under the calculation field sizes, the actual blocking rate is 2.4%, which meets the requirement that the blocking rate should less than 3%.

In a CFD simulation, it is necessary to mesh the field reasonably. In this paper, the ICEM software is used to generate structured grids. Refined mesh are considered in all directions near the surfaces of the building models with gradually and smoothly transition to avoid the effects due to sharp changes in grid density. The meshing result is shown in Fig. 3.7.

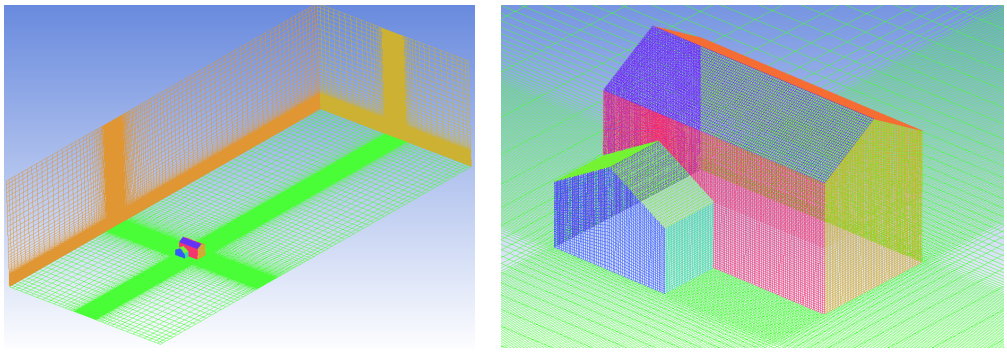

(a) Global (b) Local

Fig. 3.7 Field meshing of building models with multi-slope and multi-level roofs

3.2.3 Boundary conditions and model calculation parameters

The boundary conditions and basic parameter settings used in the CFD simulation in the study are shown in Table 3.2.

Tab. 3.2 Boundary layer conditions and basic parameter settings

Inlet boundary	Velocity-inlet Exponential average wind speed profile: $\overline{U}(z)=\overline{U}_0(\frac{z}{z_0})^{\alpha}$ Terrain category B in GB50009-2012, z_0=10m, $\overline{U}_0$=10m/s, and α=0.16 Turbulent kinetic energy: $k=1.5(uI)^2$ Turbulent dissipation rate: $\varepsilon=0.09^{0.75}k^{1.5}/l$
Outlet boundary	Outflow
Ground and walls of the calculation field	Non-slip wall
Top and both sides of the calculation field	Symmetry
Pressure-velocity coupling algorithm	SIMPLE
Difference scheme	Second order upwind
Turbulence model	Reynolds stress model

3.3 Results and analysis of wind pressure distribution on roofs

After CFD calculation, the roof wind pressure distribution of each model under various wind directions are shown and compared in Figure 3.8-3.19.

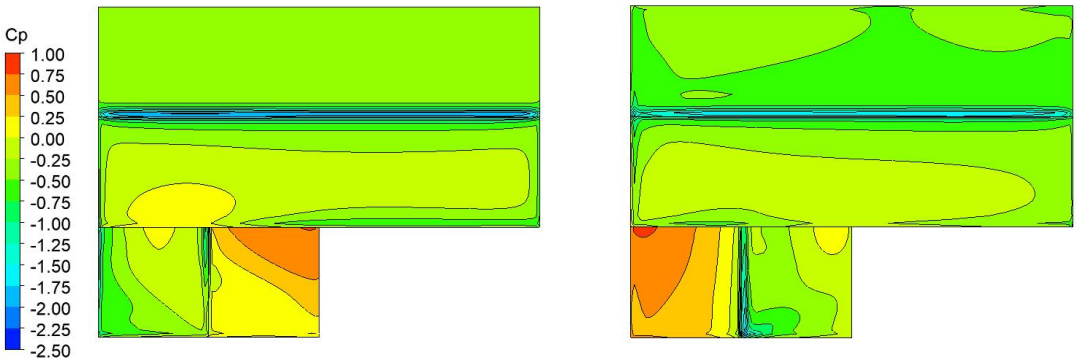

(a) 0° (b) 45°

(c) -45° (d) 90°

Fig. 3.8 Mean wind pressure coefficient on roofs of 2FP1

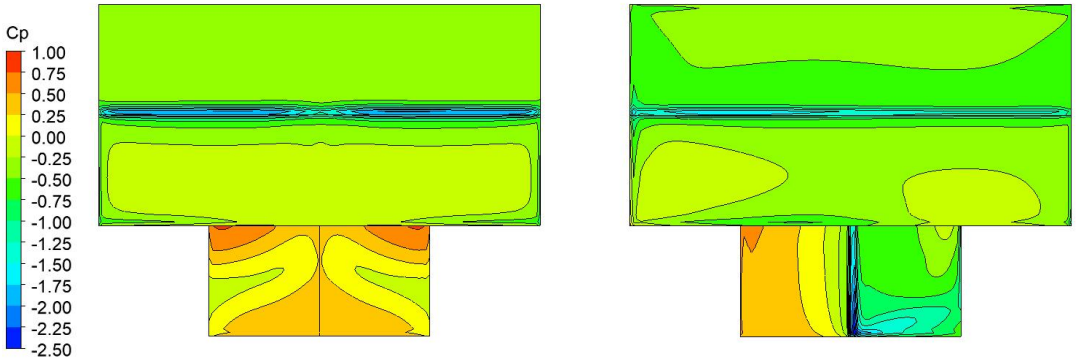

(a) 0° (b) 45°

(c) 90°

Fig. 3.9 Mean wind pressure coefficient on roofs of 2FZ1

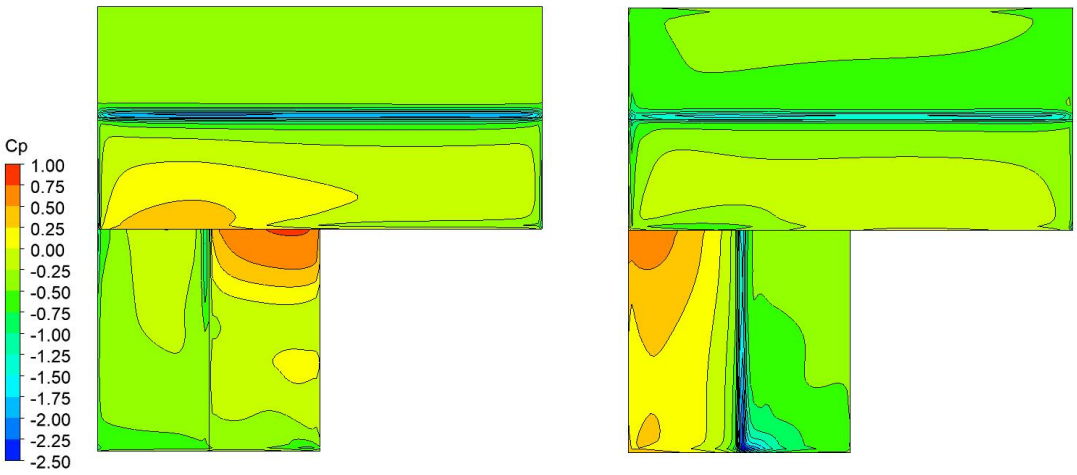

(a) 0° (b) 45°

(c) -45° (d) 90°

Fig. 3.10 Mean wind pressure coefficient on roofs of 2FP2

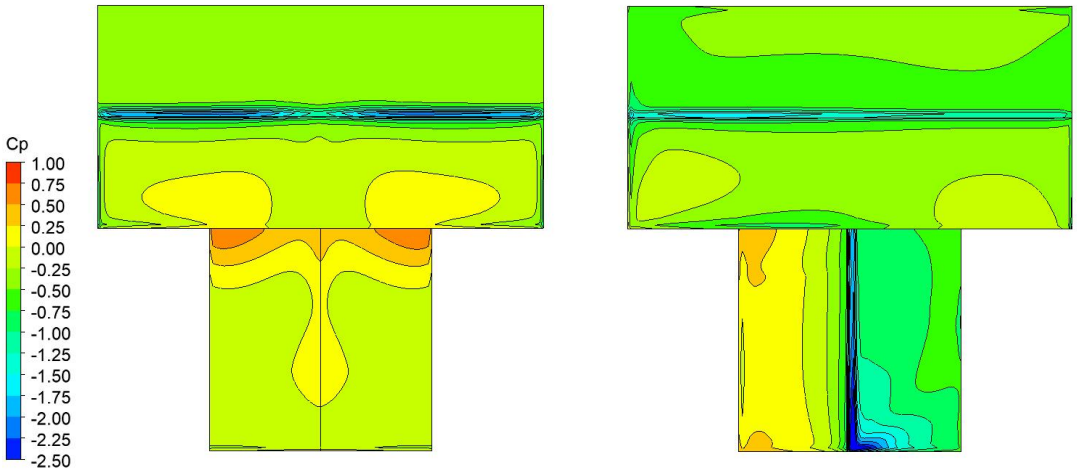

(a) 0° (b) 45°

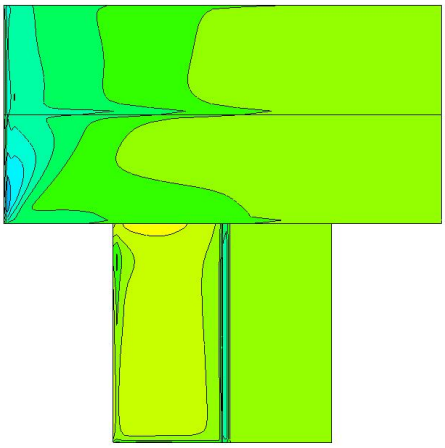

(c) 90°

Fig. 3.11 Mean wind pressure coefficient on roofs of 2FZ2

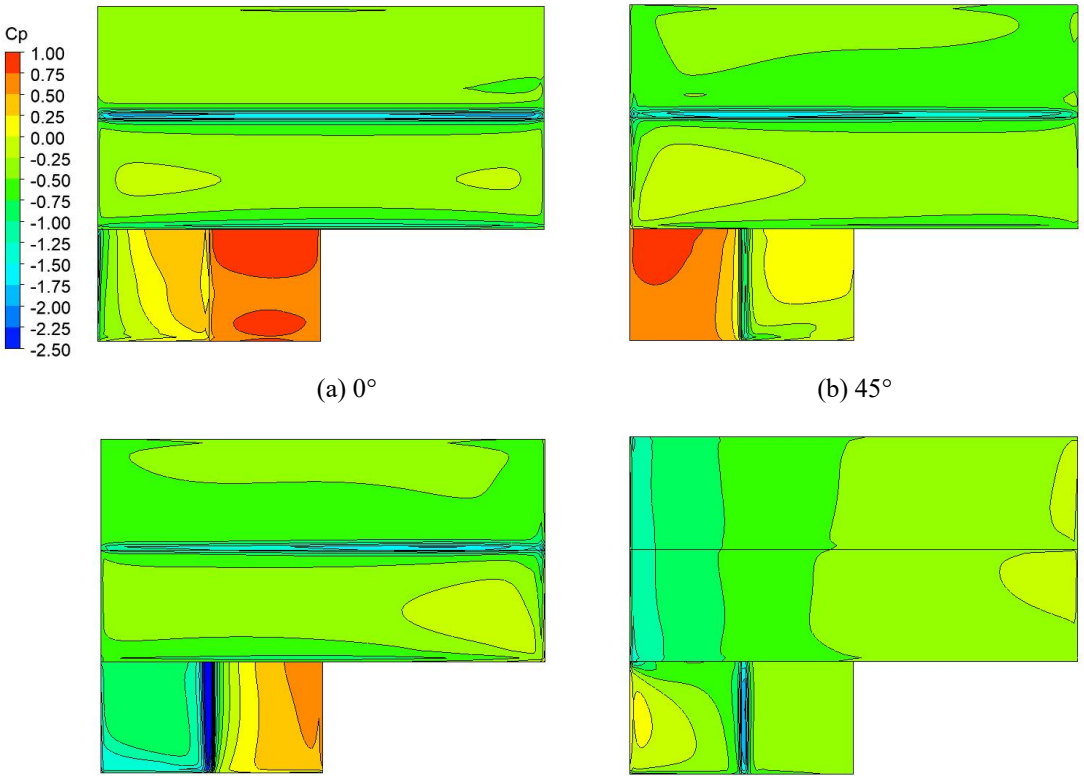

(a) 0°

(b) 45°

(c) -45°

(d) 90°

Fig. 3.12 Mean wind pressure coefficient on roofs of 3FP1

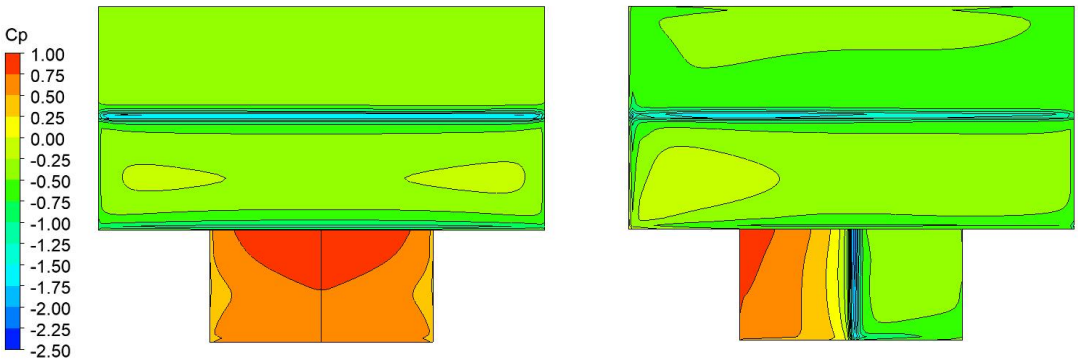

(a) 0°　　(b) 45°

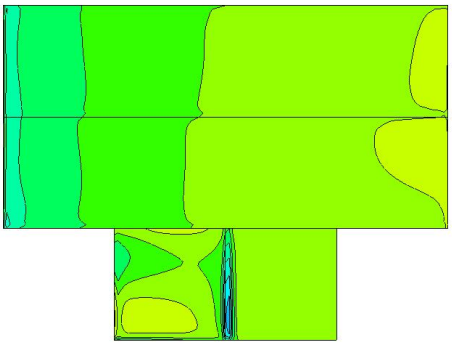

(c) 90°

Fig. 3.13 Mean wind pressure coefficient on roofs of 3FZ1

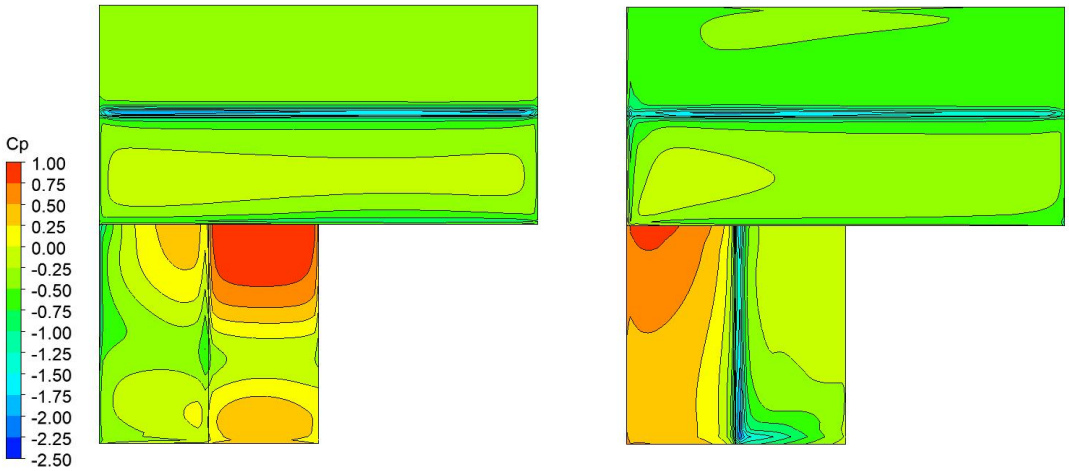

(a) 0°　　(b) 45°

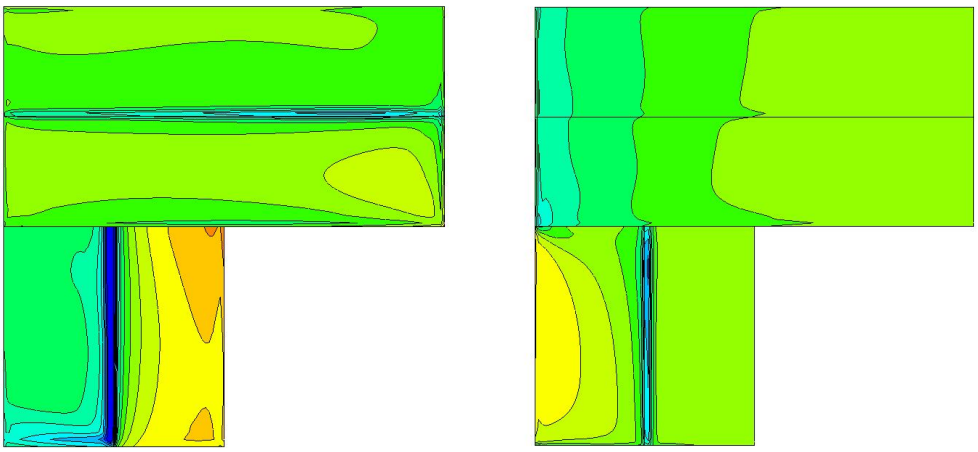

(c) -45° (d) 90°

Fig. 3.14 Mean wind pressure coefficient on roofs of 3FP2

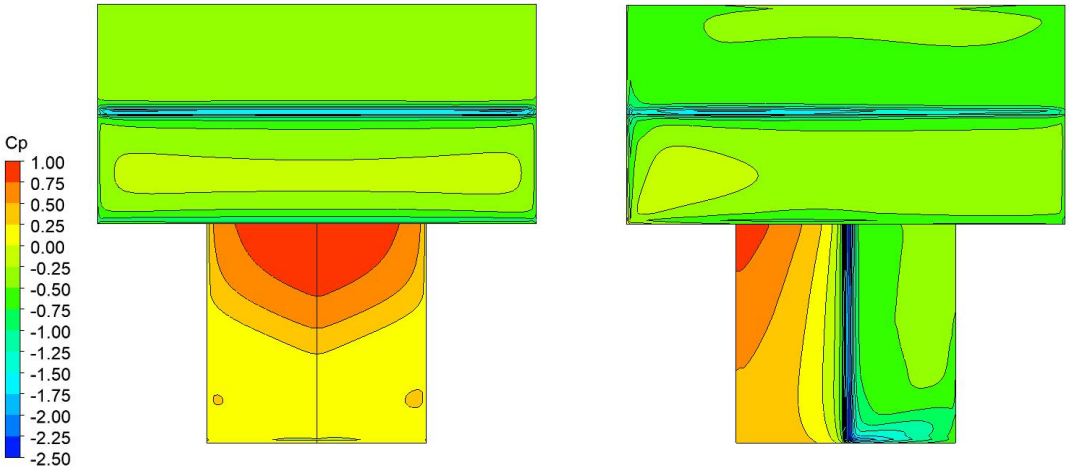

(a) 0° (b) 45°

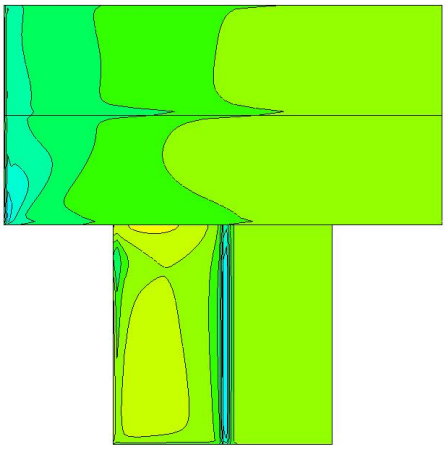

(c) 90°

Fig. 3.15 Mean wind pressure coefficient on roofs of 3FZ2

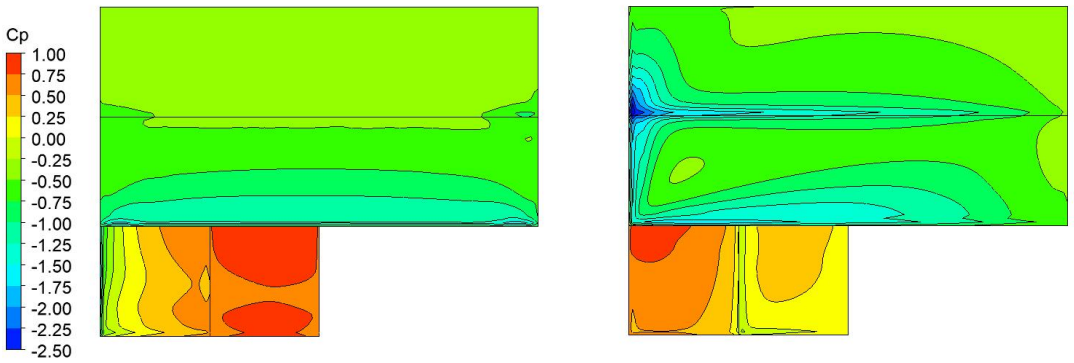

(a) 0° (b) 45°

(c) -45° (d) 90°

Fig. 3.16 Mean wind pressure coefficient on roofs of 3FP1R15

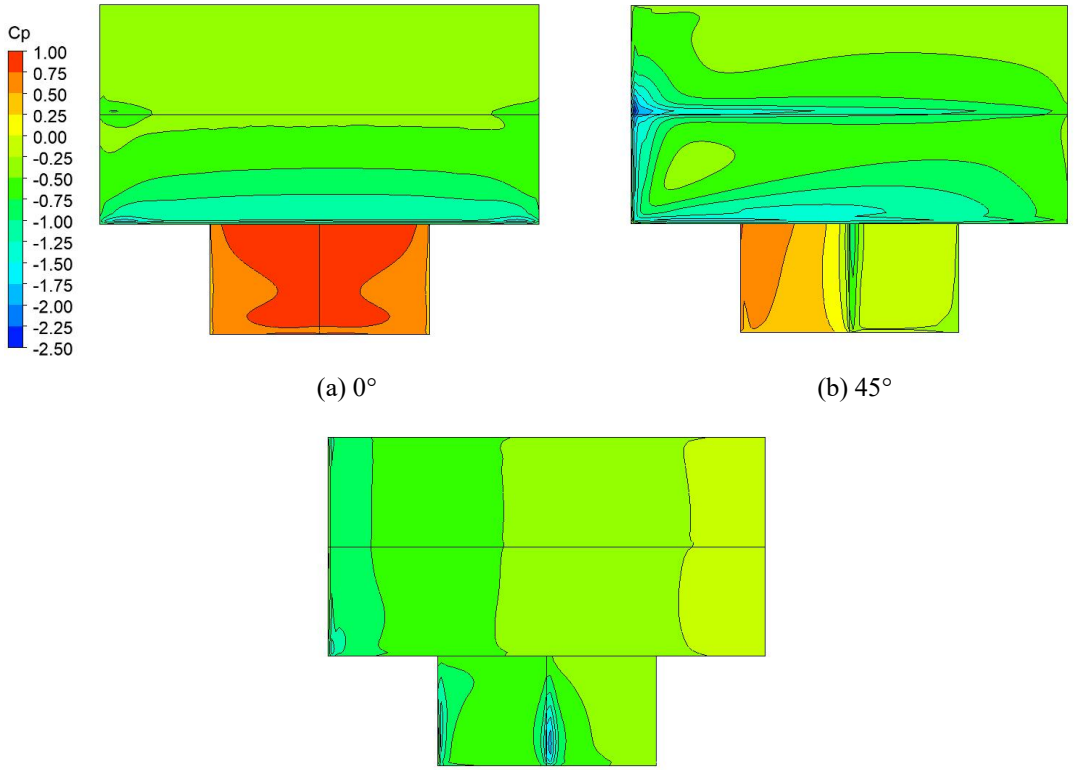

(a) 0° (b) 45°

(c) 90°

Fig. 3.17 Mean wind pressure coefficient on roofs of 3FZ1R15

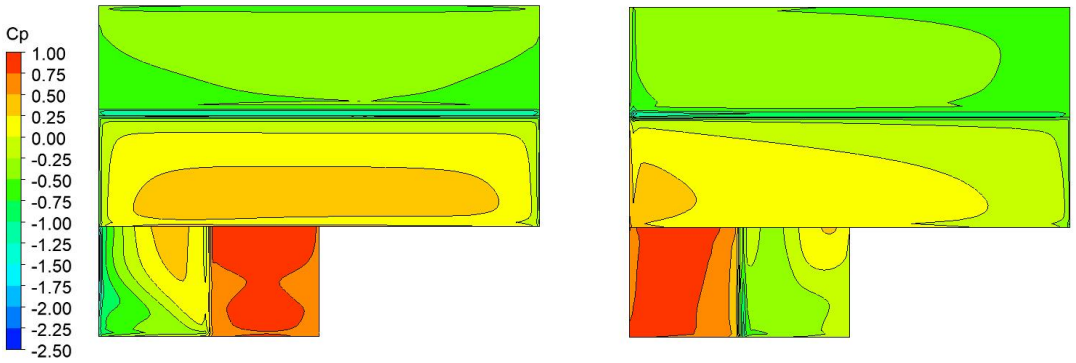

(a) 0° (b) 45°

(c) -45° (d) 90°

Fig. 3.18 Mean wind pressure coefficient on roofs of 3FP1R45

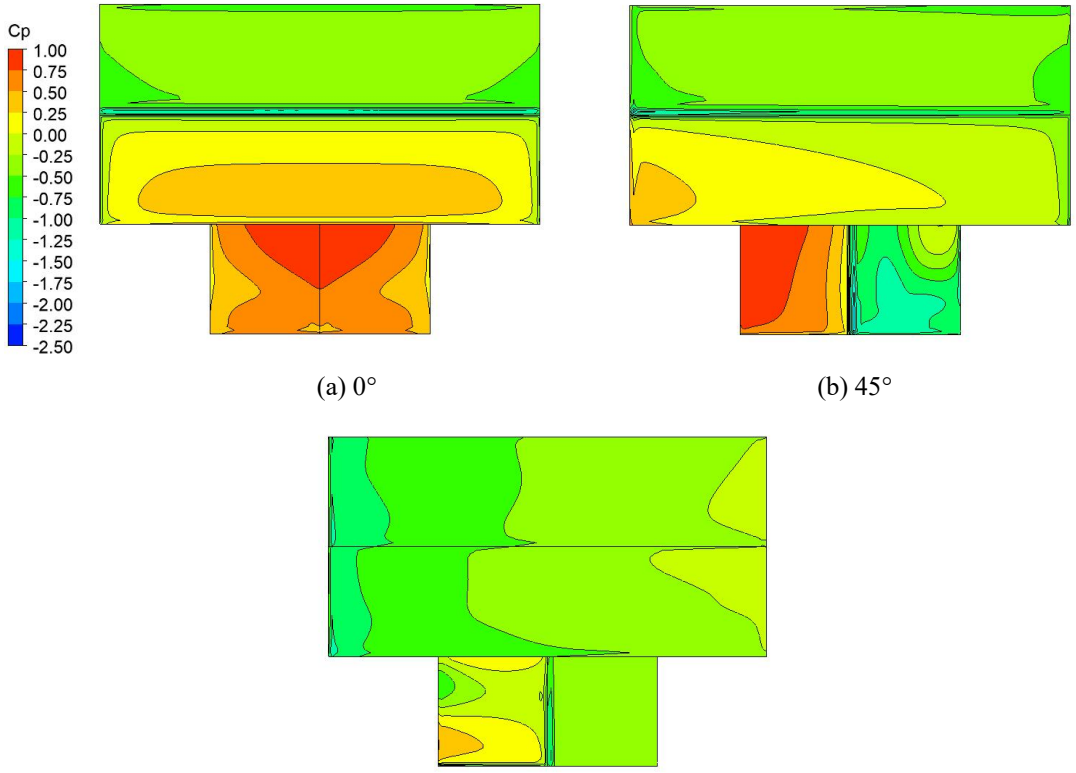

(a) 0° (b) 45°

(c) 90°

Fig. 3.19 Mean wind pressure coefficient on roofs of 3FZ1R45

According to Fig. 3.8 - Fig. 3.19, some main conclusions can be drawn as follows:

1. For the lower roof, under the 0° wind direction, the extreme positive pressure on the roof surface appears near the wall center of the higher building part, and the extreme negative pressure appears at the outer edge of the lower building part or at the windward cornice away from the higher wall. When the lower building part is offset, the roof area close to the outside bears negative pressure, and the distribution of wind pressure at the outermost area is similar to that of the simple double-slope roof model with same geometry, while the inner part of roof bears positive pressure near the windward wall of higher building part; With the increase of the height difference of roof cornice, the positive pressure of lower roof increases as a whole, the extreme positive pressure also increases, and the negative pressure on the roof decreases; With the increase of the total length of the lower building part, the wind pressure of the lower roof far from the windward wall of the higher building part is less and less affected by the higher building part, and the negative pressure gradually appears and increases; With the increase of roof slope, the absolute values of extreme positive pressure and extreme negative pressure on lower roof increase.

2. For the lower roof, under the condition of oblique wind direction, the extreme positive pressure of the roof appears near the junction of the windward cornice and the higher wall, and the extreme negative pressure appears at the windward end of the leeward roof near the roof ridge. The existence of higher building part reduces the negative pressure of the roof with downward oblique wind, and also reduces the extreme negative pressure on the lower roof. From the point of view of extreme negative pressure, the change of layout of lower building part also affects the projected area of higher building part in the downwind direction of lower building part. The larger the projected area of higher building part in the downwind direction of lower building part, the greater the height difference of roof cornices, and the smaller the extreme negative pressure generated at the end of lower roofs. With the increase of the total length of the lower building part, the end of the roof is gradually away from the higher wall, and then the extreme negative pressure increases; Under the condition of oblique wind direction, the absolute values of extreme positive pressure and extreme negative pressure on the lower roof increase with the increase of roof slope, too.

3. For the lower roof, under 90 ° wind direction, the negative pressure coefficient on the lower roof is reduced due to the obstruction of higher building part to the air flow. The variation range of wind pressure coefficient on windward roof is relatively large, but the extreme negative pressure is relatively small. The distribution of wind pressure coefficient on the leeward side is relatively uniform, generally about -0.3 ~ -0.4. Generally speaking, under this wind direction, except that the junction between the windward cornice and the higher wall needs to be paid attention to to a certain extent, the other parts can refer to the wind pressure distribution of the simple double-slope roof under the same wind direction.

4. For the higher roof, the effect on the higher windward roof is mainly reflected in the reduction of local negative pressure and the increase of positive pressure, but generally speaking, the effect on the higher roof by lower building part is relatively small, and the extreme negative pressure on the higher roof appears at the corner of the windward cornice and the end of the ridge, while the lower building

part have little effect on those areas, so the influence by the lower building part on the extreme negative pressure on the higher roof is small, It has a relatively great influence on the extreme positive pressure (or minimum negative pressure) of higher roof. The smaller the height difference of roof cornice, the greater the total length of lower building part, and the greater the extreme positive pressure in the affected area of higher roof. At 90 ° wind direction, the influence of lower building part on higher roof is minimal. At this wind direction, the wind pressure coefficient of higher roof is distributed in a trapezium shape, and the extreme negative pressure appears at the corner of windward cornice, which is the same as the extreme negative pressure of simple double-slope roof with same shape under the same conditions.

3.4 Conclusions

By means of CFD simulation, this paper analyzes effect of multi-slope and multi-level shape on wind pressure distribution on typical roofs of low-rise light-weight steel residential buildings, and discusses the influence of different parameters on the results. The main conclusions are as follows:

(1) Five turbulence models are selected to simulate the Silsoe Cube model, respectively. The CFD results of each group are compared with the field measurement and wind tunnel test results. It is found that the simulation results of Reynolds stress model are in the best agreement with the field measurement and wind tunnel test results, which is used for CFD simulation in the study.

(2) For low-rise residential buildings with multi-slope and multi-level roofs, the lower roof is greatly affected by the higher building part, and the wind pressure distribution on the lower roof varies greatly under different wind directions. The different layout of the lower building part mainly affect the extreme negative pressure at the end of the ridge, while the wind pressure distribution on the higher roof under each wind direction is much less affected by the lower building part. With the decrease of the length of lower buildings, the influence of lower buildings on the wind pressure distribution of higher roofs decreases correspondingly. With the increase of cornice height difference, the influence of lower buildings on the wind pressure distribution of higher roofs decreases. Due to the little effect of the lower building part, the higher roof can be designed according to the double-slope roof with same shape.

(3) The change of shape parameters of building models with multi-slope and multi-level roofs has a certain effect on the extreme pressure value of lower roof, but only the change of roof slope has greater effect on the wind pressure distribution for lower roof. The different layout of lower building part makes the projection area of the end area of lower roof on the wall of higher building part different along the direction of wind angle under the same wind direction. With the gradual increase of the projection area of downwind direction, the extreme negative pressure at the end of lower roof decreases gradually; With the increase of the height difference of roof cornice, the extreme positive pressure on lower roof increases and the extreme negative pressure decreases; With the increase of the total length of lower building part, the extreme negative pressure at the end of the ridge increases correspondingly because the end area of the ridge is farther away from higher building part; With the increase of roof slope, the absolute values of extreme positive pressure and extreme negative pressure of lower roof increase.

References

[1] L. Q. Yang, Y. P. Lu, X. Li. Research on low-rise residential system with fabricated light steel structure [J]. Building Technology Development, 2019, 46(6):11-12(in Chinese)

[2] X. K. Jing, Y. Q. Li. State-of-the-art: research on wind-resistant design of light-weight steel structures [J]. Sichuan Building Science, 2012, 38(03):30-34(in Chinese)

[3] Ministry of Construction of the People's Republic of China. Load Code for the Design of Building Structure: GB 50009-2012[S]. Beijing: China Architecture & Building Press, 2012 (in Chinese)

[4] Ministry of Construction of the People's Republic of China. Technical Specification for Low-Rise Cold-formed Thin-Walled Steel Buildings: JGJ227-2011[S]. Beijing: China Architecture & Building Press, 2011 (in Chinese)

[5] British Standard, BS EN 1991-1-4:2005, Eurocode 1: Actions on structures —Part 1-4: General actions — Wind actions.

[6] 日本建築学会,『 建築物荷重指針・同解説 2015 』, 丸善 (発売), 2015.

[7] ASCE/SEI 7-16, Minimum Design Loads and Associated Criteria for Buildings and Other Structures, American Society of Civil Engineers, 2016

[8] P. J. Richards, R. P. Hoxey, L. J. Short. Wind pressures on a 6m cube [J]. Journal of Wind Engineering and Industrial Aerodynamics, 2001, 89(14):1553-1564.

[9] P. J. Richards, R. P. Hoxey, B. D. Connell, et al. Wind-tunnel modelling of the Silsoe Cube[J]. Journal of Wind Engineering and Industrial Aerodynamics, 2007, 95(9):1384-1399.

4. Published Paper etc.

1. Yuan-Qi Li, Hui Wang and Akihito Yoshida, Wind pressure distribution on multi-slope and multi-level roofs of low-rise light-weight steel residential buildings, Wind-Hazard Mitigation・Wind-Resistant Construction Field Joint Open Research Meeting, Wind Engineering Joint Usage / Research Center, Tokyo Polytechnic University, February 28, 2022.

5. Research Group

1. Representative Researcher

Yuanqi Li, Professor, Dept. of Structural Engineering, Tongji University, China

2. Collaborate Researchers

1) Akihito Yoshida, Professor, Wind Engineering Research Center, Tokyo Polytechnic University, Japan.

2) Yehua Wang, Ph.D., Dept. of Structural Engineering, Tongji University, China

3) Hui Wang, MS Student, Dept. of Structural Engineering, Tongji University, China

6. Abstract (half page)

Wind Pressure Distribution on Multi-slope and Multi-level Roofs of Low-rise Light-weight Steel Residential Buildings

Yuanqi Li (Dept. of Structural Engineering, Tongji University, China)

Keywords: Low-rise building with multi-slope and multi-level roofs, CFD simulation, Mean wind pressure distribution

Abstract

This project mainly focuses on the effect of multi-slope and multi-level shape on wind pressure distribution on typical roofs of low-rise light-weight steel residential buildings. Firstly, the difference of simulation accuracy of Silsoe standard model by different turbulence models in CFD simulation is compared and discussed. By comparing the CFD simulation results of each turbulence model with the field measurement and wind tunnel test results, the most suitable turbulence model in agreement with the actual results is selected, by which the effectiveness and feasibility of the CFD simulation method in this paper are verified. Then, the typical building model with multi-slope multi-level roofs is simplified and module-based designed, and the mean wind pressure distribution of several groups of models with different shape parameters is calculated by CFD simulation. Finally, according to the CFD simulation results, the wind pressure distribution on the multi-slope and multi-level roofs, and the influence of different shape parameters on the wind pressure distribution and wind pressure value are compared and summarized, which is very helpful for further wind tunnel investigation.